

OBSERVING AND MODELLING STELLAR MAGNETIC FIELDS: BASIC PHYSICS AND SIMPLE MODELS

John D. Landstreet¹

Abstract. This and the following two chapters present a general introduction to the subject of observing magnetic fields in stars using spectropolarimetry. The three chapters will consider (1) the basic physics of the Zeeman and related effects, direct deductions about stellar magnetic fields that may be made where this effect is detected, and how such measurements have provided much information about the Sun and other magnetic stars; (2) how spectropolarimetric observations of magnetic stars may be modelled, and how such techniques may be used to extract much detailed information about the stellar magnetic field and other characteristics of the magnetized stellar atmosphere; and (3) how other magnetic effects such as the Hanle effect and continuum polarisation may be used to detect fields in a variety of stellar types such as white dwarfs, and how the current body of observational knowledge about magnetic stars may be integrated into a roughly coherent, provisional scenario of field origin and evolution.

In this chapter we survey the physics of an atom in a magnetic field (the Zeeman effect and its relatives), and identify ways in which magnetic effects on the atomic energy level structure may be used to detect and characterise stellar magnetic fields. We survey some of the basic features of magnetism in the Sun. We then describe how the available data may be used to deduce simple averages of various magnetic quantities over the stellar surface (for example, the “mean longitudinal field”) and how such simple field measurements are used to develop and explore the “oblique (dipole) rotator model” of magnetism for a group of middle main sequence stars called the “magnetic Ap stars”.

1 Introduction

This chapter and the two following chapters will present a general introduction to the observational study of stellar magnetic fields, primarily in upper main sequence

¹ Dept. of Physics & Astronomy, University of Western Ontario, London, ON N6A 3K7
Canada

and white dwarf stars. The basic questions that will be explored are the following. (1) Under what circumstances can we detect magnetic fields at the surface of stars? What observational methods are useful for this? (2) What information can we obtain about the field strength, the field structure, and related phenomena at the surfaces of stars where fields are detected or inferred? (3) Are the observations of fields in various classes of stars consistent with any overall scenario of field origin and evolution?

The plan of these chapters is to begin with a review of various aspects of the physics of an atom in a magnetic field, particularly the Zeeman effect, and to explore how such physics enables us to observe and study magnetic fields in stars. Then observations of stellar magnetism in the Sun and in upper main sequence stars (mostly in the “magnetic Ap stars”, about which the most is known) will be discussed, with emphasis on how observations can be used to obtain “direct” measurements of various kinds of average fields, and how such measurements lead to definite conceptual models of the stellar fields observed.

In the next chapter, the study of stellar fields by modelling of spectra and spectropolarimetric data is discussed. This method requires much more elaborate computational tools, but is capable of providing much more detailed information about the magnetic fields and related phenomena in stars.

Finally, in the third of these chapters, we survey some recent advances in the study of magnetic Ap stars, and then return to physics to review the Hanle effect. We next turn to the continuum polarisation produced by megaGauss fields in white dwarfs, and survey the fields found in (single) white dwarfs. The totality of data now available about fields in pre-main sequence stars, main sequence stars, and white dwarfs suggests a dichotomy between fields in low-mass main sequence stars, which seem to be produced by contemporary dynamos, and those of upper main sequence stars and their successors the magnetic white dwarfs, which appear to be consistent with retention of a global field produced rather early in the star’s history (the fossil field theory).

The subjects of these chapters have been reviewed in several recent publications. A number of useful reviews on magnetism in many classes of stars are found in Mathys et al. (2001). The connections between magnetism and stellar activity, particularly in the Sun and in low-mass stars, are discussed in Arnaud & Meunier (2003). Magnetic fields and related phenomena in upper main sequence stars are surveyed in Balona et al. (2003). The many phenomena associated with magnetism in magnetic Ap stars are reviewed in Zverko et al. (2005). The chapter by Mestel & Landstreet in Wielebinski & Beck (2005) gives a general overview of magnetism in stars, from both a theoretical and an observational perspective. Finally, Mestel (1999) provides a comprehensive view of the consequences of magnetic fields for many aspects of stellar structure and evolution. (Mestel is currently preparing a second edition of this magisterial volume.)

2 The atom in a magnetic field

2.1 General ideas

Direct detection and measurement of a stellar magnetic field is generally made possible by the effect of the magnetic field on atoms in the stellar atmosphere, which results in changes in the structure and energies of atomic energy levels, and in turn leads to observable changes in the profiles and polarisation properties of stellar spectral lines. The Zeeman effect is one example of these effects, but the influence of a magnetic field on atoms has several names in different regimes of field strength.

We start by recalling the Hamiltonian of an isolated atom in a magnetic field, here written for the case of a central potential and L-S coupling, in the Gaussian cgs units that I will use throughout:

$$H = -\frac{\hbar^2}{2m}\nabla^2 + V(r) + \xi(r)\mathbf{L} \cdot \mathbf{S} + \left[-\frac{e}{2mc}\mathbf{B} \cdot (\mathbf{L} + 2\mathbf{S}) + \frac{e^2}{8mc^2}B^2r^2\sin^2\theta \right]. \quad (2.1)$$

In this equation, of course, m and e are the electron mass and charge and c is the speed of light; \mathbf{B} is the vector magnetic field strength (magnetic induction); \mathbf{L} and \mathbf{S} are the orbital and spin angular momentum operators, and in the central field and L-S coupling approximation, the spin-orbit interaction is

$$\xi(r) = (m^2c^2/2)(1/r)(dV/dr). \quad (2.2)$$

The first three terms of the Hamiltonian are respectively the kinetic energy, potential energy, and spin-orbit coupling energy. The last two terms are the magnetic energy, derived from describing the magnetic field using a vector potential (cf. Schiff 1955, Secs 38 and 39).

For fields up to about 10 MG (megaGauss) = 1kT (kiloTesla), the magnetic terms in Eq. 2.1 are small compared to the Coulomb potential $V(r)$. In this situation one may normally treat both the fine structure produced by the spin-orbit coupling, and the magnetic splitting, using perturbation theory on states of the Hamiltonian of the central field.

For various field strengths B , the relative sizes of the spin-orbit energy and the two magnetic terms changes, leading to different perturbation treatments:

- If the (quadratic field term) \ll (linear field term) \ll (spin-orbit term), the regime is known as the (linear) Zeeman effect.
- If both (quadratic field term \ll (linear field term) and the (spin-orbit term) \ll (linear field term), the regime is known as the Paschen-Back effect.
- If the (quadratic magnetic term) \gg (linear magnetic term) and the (quadratic magnetic term) \gg (spin-orbit term), the effect is called the quadratic Zeeman effect.

It is interesting to get an idea right away of what actual magnetic field strengths lead to various regimes. To do this we need to estimate the size of the various terms in Eq. 2.1, which we do by making the substitutions $\mathbf{L} \sim \hbar$, $r \sim a_0$ (the Bohr radius of the atom), and $V \sim Ze/a_0$. We find:

- Normal atoms in fields of $B < 50$ kG (5T) are mostly described by the Zeeman effect.
- Fine structure splitting varies greatly from one atomic configuration to another, so a few spectral lines may be in the Paschen-Back limit at much smaller fields than normal. This occurs when two fine structure levels of the same term are quite close together, so that two lines of a single multiplet are very close in wavelength (say within 1 or 2 Å of each other in the visible). An example is the pair 6147.74 – 6149.24 Å of multiplet 74 of Fe II. Similarly, line splitting in H and Li I is in the Paschen-Back regime for fields below 30 kG.
- Above about 100 kG, the quadratic term becomes important. The quadratic Zeeman effect is observed in lines of H.
- In a field of more than some tens of MG the magnetic terms become comparable to the Coulomb term, and a perturbation treatment is no longer possible. In this situation one must solve for the structure of the atom in both fields together. Since the electrostatic field of an atom has spherical symmetry while a magnetic field has cylindrical symmetry, there is no natural coordinate system for this problem, and solution is really rather difficult.

2.2 The Zeeman Effect

In the Zeeman (weak-field) regime, fine structure energy levels are only slightly perturbed by the term $(e/2mc)\mathbf{B} \cdot (\mathbf{L} + 2\mathbf{S})$. If the atom is described by L-S coupling (a pretty good approximation for light atoms), J and m_J are good quantum numbers. The magnetic moment of the atom is aligned with \mathbf{J} . Since the energy of a magnetic moment in a magnetic field (think of a small bar magnet) is proportional to $\mathbf{B} \cdot \mathbf{J}$, there are $2J + 1$ different magnetic sublevels of each energy level i whose energy in zero magnetic field is E_{i0} . These sublevels are found to have energies

$$E_i = E_{i0} + g_i \left(\frac{e}{2mc} \right) B m_J \hbar, \quad (2.3)$$

where g_i is a dimensionless factor usually lying between 0 and 3 that varies from one energy level to another, and is given in L-S coupling by

$$g_i = 1 + \left(\frac{J(J+1) + S(S+1) - L(L+1)}{2J(J+1)} \right). \quad (2.4)$$

Spectral lines arise from allowed transitions between the energy levels given by Eq. 2.3, with $h\nu_{ij} = E_i - E_j$. This gives rise to a set of closely spaced frequencies

Zeeman components for sodium D lines

green: pi components, red & blue: sigma components

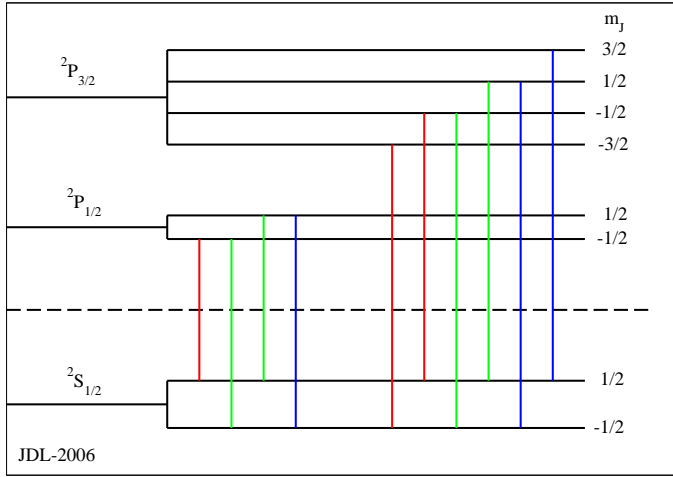


Fig. 1. Zeeman splitting of the Na D doublet in a magnetic field.

given by

$$\nu_{ij} = \frac{E_i - E_j}{h} = \nu_0 + \left(\frac{e\hbar B}{2mch} \right) (g_i m_i - g_j m_j), \quad (2.5)$$

where the selection rule is that $m_j = m_i \pm 0, 1$. The corresponding component wavelengths are

$$\lambda_{ij} = \frac{c}{\nu_{ij}} = \lambda_0 + \Delta\lambda_Z = \lambda_0 + \left(\frac{e\lambda_0^2 B}{4\pi mc^2} \right) (g_j m_j - g_i m_i), \quad (2.6)$$

where numerically, with λ in \AA and B in G,

$$\Delta\lambda_Z(\text{\AA}) = 4.67 \cdot 10^{-13} \lambda_0^2 B (g_j m_j - g_i m_i). \quad (2.7)$$

Notice that the line splitting is proportional to B and to λ^2 .

An important constraint on the components into which a single line splits in the presence of a magnetic field is furnished by the selection rules, requiring $m_j = m_i$ (called pi components) or $m_j = m_i \pm 1$ (called sigma components). Only some combinations of the sublevels into which each energy level splits produce actual lines. As an example, the Zeeman components of the sodium D lines at 5889, 5895 \AA are illustrated in Fig. 2.2. Notice that no allowed transition occurs between the $m_J = +3/2$ sublevel of the ${}^2P_{3/2}$ level to the $m_J = -1/2$ sublevel of the ${}^2S_{1/2}$ level.

The actual size of the line splitting is about $\pm 0.012 \text{\AA}$ (pi-sigma separation) for a transition at 5000 \AA in a field of 1 kG.

A special case occurs if the spacing of the upper energy sublevels is the *same* as the spacing of the lower energy sublevels. In this case, all the line components produced by the same value of $\Delta m_J = m_j - m_i$ have the same wavelength (i.e. they overlap), and only three line components are observed. For historical reasons, this case is called the “normal Zeeman effect”. Usually, however the spacing of upper and lower levels is different (as in Fig. 2.2), and a larger number of line components appear. (This case is sometimes called the “anomalous Zeeman effect”.)

A few specific lines have no splitting (some combinations of J , L and S , for example $^4D_{1/2}$, can lead to a value of $g_i = 0$ in Eq. 2.4, or one of the levels can have $J = 0$, which means that m_J in Eq. 2.3 is identically zero). Such lines are called “null lines” and are valuable aids to assessing line width due to factors other than magnetic splitting or broadening.

Splitting of each energy level is determined by the Landé factor g_i . The best experimental values have mostly been assembled by Charlotte Moore in three volumes as National Bureau of Standards Circular 467 (1949; 1952; 1958). A large number of Landé factors have been computed by R. L. Kurucz. Both these resources, and many others, are incorporated into the on-line Vienna Atomic Line Database (VALD: <http://ams.astro.univie.ac.at/vald/>). In the absence of better data, however, calculated g_i values using L-S coupling (Eq. 2.4), or equivalent expressions for other coupling schemes as appropriate, usually provide useful estimates.

2.3 The Paschen-Back Effect

The Paschen-Back effect has few astronomical applications in non-degenerate stars, although it is relevant for analysis of some of the weakest fields found in magnetic white dwarfs. The fields found in main sequence stars (generally of the order of 1 kG, very rarely as large as 30 kG) are not large enough to push most lines out of the Zeeman regime into the Paschen-Back regime.

However, a few levels have abnormally small fine-structure separation, and lines produced by transitions which involve such levels have splitting which is neither pure Zeeman splitting nor pure Paschen-Back splitting, but are an intermediate case known as “partial Paschen-Back splitting”. An example is furnished by the $b^4D_{1/2}$ and the $b^4D_{3/2}$ energy levels of Fe II at 3.87 eV above ground; transitions between these levels and the $z^4P_{1/2}^o$ level lead to the two lines 6147.74 and 6149.24 of multiplet 74 which easily move into the transition regime for field strengths found in some main sequence stars.

In the Paschen-Back regime, \mathbf{L} and \mathbf{S} decouple, so J is no longer a good quantum number. Instead, the good quantum numbers are m_L and m_S , and the energy perturbation due to the magnetic moment associated with the orbital and spin angular momenta separately is given by

$$E_i = E_{i0} + \frac{e}{2mc} B(m_L + 2m_S)\hbar. \quad (2.8)$$

With this perturbation, the *separation* between adjacent levels ($eB/2mc$) is the

same for all levels, and with the selection rule of $\Delta m_L = m_{Lj} - m_{Li} = 0, \pm 1$, all lines are split by the same amount, and we observe the “normal Zeeman triplet”.

2.4 Polarisation properties of Zeeman line components

Another interesting property of the Zeeman components into which a spectral line splits when the atom is immersed in a magnetic field is that the various components have distinctive *polarisation* properties. These turn out to be very important in practice.

“Natural” light may be thought of classically as being made up of short wave trains that have no particular phase or plane of polarisation. However, by the use of suitable “polarising” devices (such as sheet Polaroid, or reflection from a dielectric surface at a suitable angle), it is possible to force electric vectors of the wave trains to vibrate in a single plane. Such light is called “linearly polarised”, and the plane of the electric vector is the “plane of polarisation”.

If such linearly polarised light is forced to travel through an anisotropic but transparent medium (such as a sheet of mica or a suitably orientated crystal quartz plate) which has the property that waves linearly polarised in one plane (the “fast axis”) travel a little faster than waves polarised in a plane at 90° to the first plane (the “slow axis”), a wave with a plane of polarisation at 45° to both fast and slow axis will effectively be resolved into the sum of two linearly polarised waves, one travelling with its electric vector parallel to each of the crystal axes. If the speed of travel of these components were the same along both axes, when the wave train emerged from the crystal the two component waves would have the same phase relation as when they entered, so the linearly polarised wave we are considering would remain linearly polarised in the original plane.

However, if the difference in wave velocity and the thickness of the plate are adjusted so that one of the two components is retarded by one-quarter cycle with respect to the other component, the emerging wave has a new kind of polarisation: “circular polarisation”. In this state, if we look at the direction of the electric vector at an instant all along the wave train, it follows a spiral form in space. Alternatively, if we look at the wave at one point in space as it varies in time (for example at the point where it emerges from our anisotropic crystal, or “quarter wave plate”), the fact that the two orthogonal components into which we have resolved the wave are now 90° out of phase means that the wave vector *rotates* once per wave period (hence the term “circular polarisation”).

The various Zeeman components into which a spectral line splits when the atom is in a magnetic field are polarised. This polarisation depends on the orientation of the field with respect to the direction of the emitted light. Two simple cases occur.

If the field is perpendicular to the line of sight, then transitions with $\Delta m = 0$ (π components) are linearly polarised with their electric field vectors parallel to the field lines. Transitions with $\Delta m = \pm 1$ (σ components) are linearly polarised perpendicular to the field.

If the field is aligned parallel to the line of sight, the line components produced

by $\Delta m = 0$ transitions vanish (they have zero intensity), while the transitions for which $\Delta m = 1$ and -1 have opposite senses of circular polarisation.

Intermediate field orientations lead to elliptical polarisation of the light from the various Zeeman components.

The quantum mechanics of multi-electron atoms, including the Zeeman effect, is described with the aid of simple classical models in Eisberg & Resnick (1985). A more advanced discussion, again with a reasonable emphasis on the physics of multi-electron atoms, is found in Bransden & Joachain (1983).

3 Detecting and measuring stellar magnetic fields

3.1 *The magnetic field(s) of the Sun*

The physics discussed so far is enough to allow us to detect a magnetic field in a star and to estimate its strength.

As we will discuss in more detail below, the fact that individual Zeeman components of a magnetically split spectral line emit polarised light also means that these same components absorb only light of specific polarisation. For example, with a longitudinal field, the sigma component of a spectral line that emits right circularly polarised light also absorbs right circularly polarised light while having no effect on left circularly polarised light. This means that at the wavelength of this sigma component, more radiation exits the star as left circularly polarised light: there is a net left circular polarisation at that wavelength, and correspondingly, net right circular polarisation at the wavelength of the other sigma component.

The first magnetic field discovered in any star occurred with the detection of the magnetic field of a sunspot by Hale (1908). Small regions on the solar surface were already being observed with high spectral resolution, and it had been noticed that spectral lines in sunspots are noticeably broadened, and at sufficiently high resolution actually split into multiple components. Hale hypothesized that the splitting is magnetic, and confirmed his idea with the aid of a circular polarisation analyser by showing that the line components in the red and blue components of the spectral line are circularly polarised in opposite senses, exactly as expected from the Zeeman effect. From the separation of the outer line components, Hale was able to estimate that the sunspot field producing the splitting was about 3000 G (about 0.3 T). Notice that even in this first detection of a stellar magnetic field the polarisation properties of the Zeeman effect played a critical role.

Hale's discovery initiated the study of sunspot magnetic fields, which blossomed during the next 50 years (see for example Bray & Loughhead 1964). A number of general characteristics of sunspots and of their occurrence on the Sun have been identified from these studies.

- Sunspot fields are typically between 1 and 3 kG. The field strength drops off to a much smaller value (at least as averaged over many thousand km on the solar surface) outside the sunspot.

- Sunspots tend to come in pairs of opposite magnetic polarity, which are usually aligned in a roughly east-west direction on the solar surface. At any one time, in one hemisphere of the Sun the leading sunspot of a pair tends to have one specific polarity (say, north polarity), while in the opposite hemisphere, the leading sunspots have the opposite polarity (say, south).
- During a roughly 11-year period, sunspots (which individually usually last for some months) are formed at first about $30^\circ - 40^\circ$ from the equator. As time goes on they appear closer and closer to the solar equator. As the sunspot production regions approach the equator, the production of sunspots dies out.
- When the next 11-year cycle starts, the sign of the magnetic field of the leading sunspots in each hemisphere has changed. Thus if the leading sunspots in the northern hemisphere had north polarity during one cycle, during the next cycle they usually have south polarity. The real period of the solar cycle is thus approximately 22 years rather than 11.
- The Sun displays numerous other variable localized features (flares, filaments, coronal loops, plages, etc) which collectively are referred to as “solar activity”. The amount of this activity is roughly proportional to the number of sunspots visible at one time.

In the 1950’s magnetic fields began to be detected over the full solar disk. This general solar magnetic field has been found to be highly intermittent, both spatially and temporally. It seems to be concentrated in small magnetic flux ropes (of which the sunspots can be regarded as the largest examples), which emerge from below the surface, move about with large-scale convective flows of various scales, and vanish again. The global magnetic field of the Sun has a loose dipolar organisation, with much emerging flux in one hemisphere and returning flux in the other. This overall pattern, like the sign of leading sunspots in one hemisphere, reverses every 11 years, again confirming that the fundamental period of solar variation is 22 years.

The magnetic fields of the solar surface are responsible for all forms of solar activity. The solar photosphere looks fairly bland and unstructured in white light, apart from the sunspots, but as one looks higher, up into the chromosphere and corona, the outer solar atmosphere becomes very highly structured and complex. This complexity is very clear in an image of the solar corona at X-ray wavelengths obtained by the Yokoh satellite (Fig. 3.1). All this complexity is controlled by the solar magnetic field.

3.2 *Detection of fields in other stars*

For nearly 40 years after the first detection of the solar magnetic field, no further fields were found in any other stars. Why not? Basically because the sunspot fields satisfied some very special conditions.

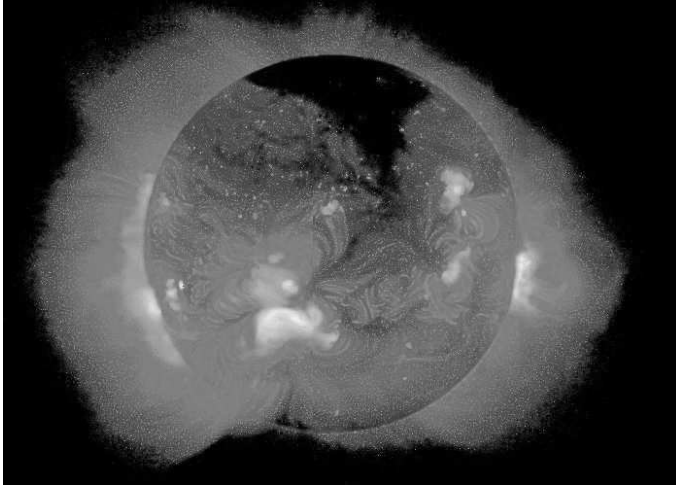


Fig. 2. Solar corona as seen in Xrays. The complex structure of dense and rare gas and of temperature variations (which determine the brightness at various points above the dark solar surface) is completely controlled by the magnetic field of the Sun.

- The Sun is very bright, so high dispersion spectroscopy was possible on the solar spectrum long before photographic emulsions were sensitive enough to make this possible on other stars.
- The Sun rotates very slowly, and sunspots are quite localised on the solar disk. Spectral lines from sunspots are not broadened at all by rotational Doppler broadening.
- The fields of sunspots are relatively strong, strong enough to produce visible splitting of the very narrow spectral lines.

Zeeman splitting in stars is quite small (of the order of 0.01 \AA per kG); even very small rotation velocities can mask this completely. (For line splitting to be detectable in a typical stellar spectral line, very roughly the field in kG must be larger than the projected rotation velocity in kms^{-1} .) Such splitting was not observed in any of the relatively bright stars that could be studied at high dispersion in the 1930's and 1940's.

Stellar fields were finally discovered by Horace Babcock, who had the clever idea of exploiting the polarisation properties of the Zeeman effect to improve the sensitivity to weak magnetic fields. He equipped the coudé spectrograph of the Mount Wilson 100-inch telescope with polarising optics. Let's see why this was such an interesting new tool.

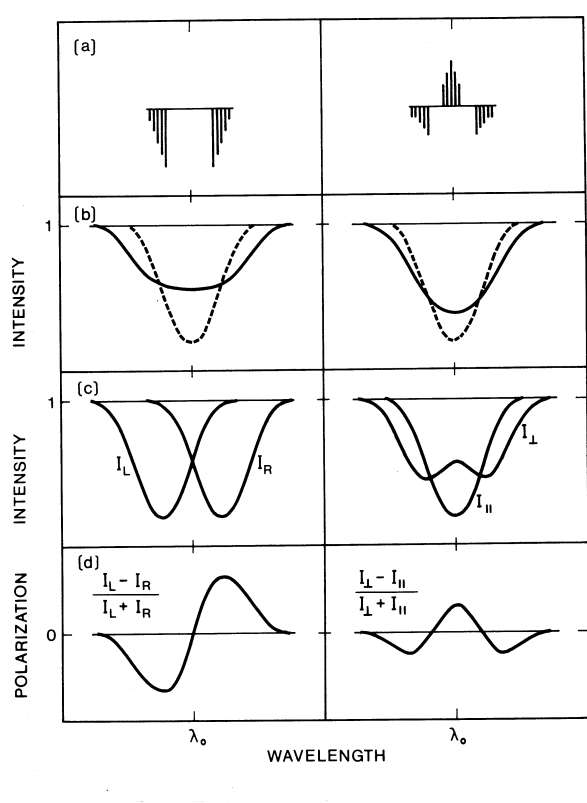


Fig. 3. Effects of Zeeman splitting and polarisation on stellar spectral lines. The right column shows the situation for a magnetic field normal to the line of sight; the left column is for a magnetic field parallel to the line of sight. The top row shows the apparent laboratory splitting. The second row compares the non-magnetic line (dotted) to the line profile with the applied magnetic field (solid). In the third row are shown profiles as viewed through right and left circular analysers (left) or linear polarisers aligned parallel and perpendicular to the field. The bottom row shows fractional polarisation signals derived from the row above.

3.3 Observing polarisation in stellar spectral lines

The effects of a magnetic field on a stellar spectral line are sketched in Fig. 3.3. In the top row, the laboratory splitting of a spectral line is shown (in the usual notation with pi components above the line, sigma components below, and component line lengths showing relative intensity). The second row shows how a stellar line profile in a non-magnetised atmosphere (dotted) would change when a magnetic field is introduced: the Zeeman splitting basically broadens the line, somewhat more if the field is along the line of sight (so that all the visible components are

offset from the line position in zero field) than if the field is normal to the line of sight. The line broadening is significant, of course, only if the Zeeman splitting is comparable to the width of the line produced by other broadening agents such as thermal and rotational broadening. Often the dominant broadening is by rotation. Notice that the broadened line is not very different from a line broadened a little more by rotation; to securely detect a field using line broadening, one must see actual line *splitting* or detect a correlation between line width and the pi-sigma component separation of the atomic Zeeman pattern, which varies by a factor of order two or three among common spectral lines.

The third row shows the spectral line as observed through a polarising filter passing only one of left or right circularly polarised light (left column) or light linearly polarised parallel or perpendicular to the field direction on the sky (right column). If instead of a single spectrum, *two* spectra are obtained, observed through the two polarising filters of either the left or right panel, the differences in line profiles as seen in the two spectra provide information about the field. The left column is especially interesting: the spectral line as seen in left circularly polarised light is not at the same wavelength as the right circularly polarised light. This means that field detection may be achieved by measuring the radial velocity *difference* between the positions of the line profile in left and right circularly polarised light, something which can be done with a precision much better than the line width. Thus fields small enough not to change the *intensity* profile of the line very much can nevertheless produce easily detectable signals. This result has been the key to most of the magnetic field detections in stars.

3.4 Discovery of fields in main sequence stars

Babcock (1947, 1958a, 1958b) searched for magnetic fields by obtaining circularly analysed spectra of various types of stars. He did this essentially by placing a quarter-wave plate in the light beam of the telescope, followed by a linear polarisation beam-splitting analyser. The effect of the quarter-wave plate is to convert circularly polarised light into linearly polarised light. Right circularly polarised light becomes linearly polarised light of one orientation, while left circularly polarised light is converted into light linearly polarised at right angles to the light that was formerly right circularly polarised. Thus light initially entering the telescope as right or left circularly polarised light remains in a distinctive (but now linear) polarisation state.

The light beam is then passed through a calcite plate (or a Wollaston prism). These devices have the effect that they make the light of two orthogonal linear polarisations follow *different paths*, so the two linear polarisation states emerge from the analyser moving along slightly different axes (or in slightly different directions). The two separated beams are then focussed on the slit of a spectrograph. Effectively there are now two star images on the slit, one of which carries the light that was left circularly polarised as it left the star, and the other of which was right circularly polarised. These two star images then pass through the spectrograph and form two parallel spectra on the detector. The simplest method of detecting

the field is then to measure the radial velocity difference between lines as seen in these two spectra, as illustrated in the third row, left column of Fig. 3.3. If the signal in a single line is weak (the radial velocity difference is very small) a more precise measurement may be obtained by averaging over many spectral lines.

Babcock restricted his search to stars having sharp spectral lines (projected rotational velocities $v_e \sin i$ of less than 20 or 30 km s^{-1}). This is because the small radial velocity differences between the lines as seen in spectra of the right and left circularly polarised light is much easier to measure if the spectral lines are narrow than if they are broad. Starting in 1947, he discovered the Zeeman polarisation signature of a magnetic field in a number of middle main sequence stars belonging to a type of unusual objects classified from their spectra as “peculiar A stars”. These are stars which appear similar to normal A and late B main sequence stars, but (a) show spectral lines of abnormal strength or weakness of various elements compared to the lines of typical A and late B stars (Si, Cr, Ti or rare earth lines might be unusually strong, He lines might be very weak), and (b) have $v_e \sin i$ values that are usually less than about 60 or 80 km s^{-1} , compared to values of 200 or 300 km s^{-1} which are usually found in A and B stars.

Clear illustration of how the measurements were done is found in Babcock (1958a, Figs. 1 & 2; but be sure to consult a printed edition of this article if possible, as the ADS on-line copy of Fig. 2 is nearly black).

Note that Babcock (1958a) thought that he had detected weak fields (of order $1 - 2 \cdot 10^2$ G) in several other categories of stars, but that most of these measurements turn out to have larger uncertainties than originally estimated, and the detections have not been confirmed.

4 Measuring and modelling Ap star magnetic fields

Once Zeeman splitting is detected in the spectra of an Ap star, the next problem is to turn measurements of spectral line shifts between the spectra of right and left circularly polarised light into useful information about the strength and distribution of the magnetic field over the stellar surface, and potentially even as a function of depth in the atmosphere. The basic idea of how to do this was introduced by Babcock, who showed that the separation between the average position of a spectral line as seen in the spectra of right and left circularly polarised starlight is approximately proportional to the line-of-sight component of the stellar field, (suitably) averaged over the hemisphere of the star that is visible at the time of observation. Thus one can go from a *measurement* of wavelength shift between the positions of a spectral line in the spectra of right and left polarised light to the *deduction* of an important characteristic of the field present on the visible stellar hemisphere, namely the average of the line-of-sight field component over that hemisphere. This does not describe the magnetic field fully, but at least it provides one very useful kind of information about the field.

Several such relations have been found that are useful for going directly from some measurement on spectra to some average (or moment) of the field over the visible hemisphere of the star. These relationships have made it possible to develop

simple models of the magnetic field geometry of Ap stars. As we shall see, these models are not exact but do contain much useful information about the global nature of the fields observed.

Two particular relationships between measurements and average field strength, the weak-field approximation and the weak-line approximation, have both been found to be very useful in estimating the mean line-of-sight (or mean longitudinal) magnetic field component, often called $\langle B_z \rangle$. Both of these relationships require measurements of spectra of right and left circularly polarised starlight. Measurement of actual line splitting, in those few stars that have large enough fields combined with small enough rotational line broadening, provide a different type of field average. In this case, one can estimate the mean value of the absolute value of the field strength $\langle |B| \rangle$, often called the mean field modulus or mean surface field, B_s . Measurement of B_s requires only a single (intensity) spectrum that is not analysed for polarisation.

4.1 The weak-line approximation

In an optically thin gas producing emission or absorption lines in a magnetic field B , the separation between the sigma and pi components of a triplet line is given by Eq. 2.7,

$$\Delta\lambda_{\sigma-\pi} = z \frac{\lambda^2 e B}{4\pi m c^2} = 4.67 \cdot 10^{-13} z \lambda_0^2 B, \quad (4.1)$$

where z is the effective Landé factor of the line. Looking at Fig. 4.1, it is plausible that when we observe a split spectral line through (say) a right circular polariser, as the inclination of the field varies from transverse to longitudinal (the angle θ between the field and the line of sight varies from $\pi/2$ to 0), the shift of the centroid of the line is given by $\Delta\lambda_{\sigma-\pi} \cos\theta$. If we observe the same line through a left circular polariser, the centroid of the transmitted line is $-\Delta\lambda_{\sigma-\pi} \cos\theta$. If we observe the spectral line simultaneously in both right and left circularly polarised light, the separation of the line centroids as seen through the two polarisers will be $\Delta\lambda = 2\Delta\lambda_{\sigma-\pi} \cos\theta$.

Therefore, if we observe the spectrum of a magnetic star in both senses of circularly polarised light, and *measure* the wavelength shift $\Delta\lambda$ between the centroids of a line as seen in left and in right circularly polarised light, we can solve the equation above to *derive* a value for $B \cos\theta$. Clearly, if the spectral line used is formed over the whole visible hemisphere of the star, the field strength derived is a hemispheric average of the line-of-sight component of the field, precisely the quantity we have been calling $\langle B_z \rangle$. And of course using many lines and averaging the result improves the precision of the measurement.

The weak-line expression is accurate only for optically thin (or weak) lines, but it provides a reasonable first approximation for strong lines as well, and it is common to use it on all measured lines regardless of strength.

Notice that unless we know exactly how the contribution to the spectral line varies over the stellar surface, we do not know exactly how the value of $\langle B_z \rangle$ is

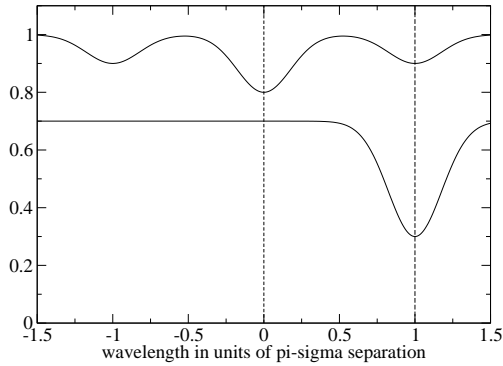


Fig. 4. The two curves in the figure show a fully Zeeman split spectral line as viewed through a circular polarisation analyser that passes only one sense of circular polarisation. The upper curve shows the line formed in a magnetic field perpendicular to the line of sight, so that all three (normal) Zeeman components are visible. The lower curve (which is shifted downward by 0.3 for visibility) shows the same line as it appears with the magnetic field parallel to the line of sight, so that the central pi component vanishes and only one sigma component is visible. In the case of transverse field the centroid of the profile is at wavelength 0, while for the longitudinal field the centroid is at +1. For intermediate field inclinations the centroid shifts as $\cos \theta$, where θ is the angle between the field and the line of sight.

weighted from centre to limb. This is a common problem with all field moments derived from simple line measurements.

4.2 The weak-field approximation

If, in addition to being weak, the spectral line as seen in right and left circularly polarised light is shifted by much less than its (local) width, a further approximation is sometimes useful (for example in measurements with Balmer lines; see Landstreet 1982 and Bagnulo et al. 2002). This approximation relates the circular polarisation as measured directly in one wing of the spectral line to $\langle B_z \rangle$. Consider Fig. 4.2. We have already seen that measurement of $\Delta\lambda$, the separation between the mean position of a spectral line as seen in right and left polarised light, may be used to determine $\langle B_z \rangle$. This separation may be determined by observing the full spectral line profile in each polarisation, but sometimes it is observationally more convenient (for example when using a polarimeter equipped with a narrow band interference filter) to measure the circular polarisation at only one or two points on the line profile. Such a measurement, together with a scan of the line profile, can also provide a value for $\Delta\lambda$.

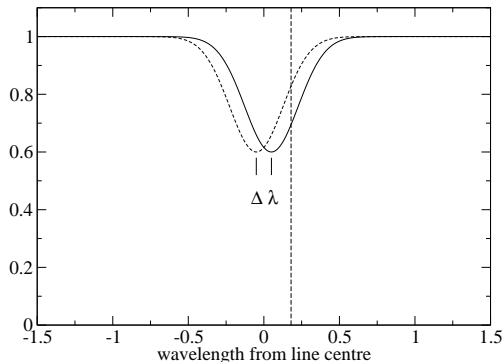


Fig. 5. A spectral line, slightly split by the Zeeman effect, as observed in right (solid line) and left (dotted line) polarisation. The circular polarisation is measured in the line wing at the position indicated by the vertical long-dashed line.

If we know the slope $dI/d\lambda$ of the line profile at the wavelength where the circular polarisation is measured (the vertical dashed line in Fig. 4.2), clearly the vertical separation between the two profiles there is given approximately by $I_L - I_R = (dI/d\lambda)\Delta\lambda$. Since the fractional circular polarisation measured at that point with a polarimeter will be $V = (I_L - I_R)/(I_L + I_R) = (dI/d\lambda)\Delta\lambda/(I_L + I_R)$ from a measurement of V and the line profile $I(\lambda)$ we can solve for $\Delta\lambda$ which in turn provides an estimate of $\langle B_z \rangle$ as in the previous section.

4.3 Basic characteristics of magnetic Ap stars

Using one or another of the methods discussed above, measurements of $\langle B_z \rangle$ have been made for more than 100 Ap stars. In many cases several or even many measurements are available for a star. When these data are examined, we find the following regularities.

- The value of $\langle B_z \rangle$ is usually variable. The variations are always periodic, and are almost always sinusoidal. Usually $\langle B_z \rangle$ reverses sign during the variation.
- Almost all the magnetic Ap stars also vary in brightness, by a few percent, with the same period as the magnetic variations.
- Most magnetic Ap stars show variations in spectral line shape and strength. The lines of each element all show rather similar variations, but different elements may show quite different variations (one element's lines may be strongest when the lines of another element are weakest, for example). Again, the period of variation is the same as that of field and light.

- The period of variation may have any value between about 0.5 d and many years. There is no obvious difference between variations with a short period and those occurring with a long period. On the other hand, the period is closely related to $v_e \sin i$: stars with long periods invariably have small $v_e \sin i$ values, while stars with large $v_e \sin i$ always have short periods.
- These facts together clearly show that the period of variation is the *rotation* period of the star, and in fact it is found that the observed periods and $v_e \sin i$ values are consistent with main sequence radii of the stars, using the elementary relationship $v_e \sin i = 2\pi R \sin i / P$. This relationship may be used to derive $\sin i$ if the radius R is accurately known (for example for stars for which distance and effective temperature are precisely determined).
- Apart from the periodic variations due to rotation of a non-axisymmetric field and abundance structure, the fields seem to be quite stable, and there are no hints yet of changes in the abundance distributions. The only irregularity seems to be that a very small number of magnetic Ap stars are apparently slowing down very gradually.

Typical variations of a magnetic Ap star are illustrated in Fig. 4.3.

The sinusoidal variations of $\langle B_z \rangle$, usually with a reversal of sign, suggests that we are seeing the rotation of a roughly dipolar field, which is inclined to the rotation axis of the star. This means that as the star rotates, we (for most stars) see first one magnetic pole and then the other. The variations in spectral line profile and strength strongly suggest that the chemical composition varies over the surface of a magnetic Ap star: the star has “abundance patches”. These abundance patches are presumably the cause of light variations (for a very nice confirmation of this, see Krťička et al. 2007). This model, of a star with a simple magnetic field structure whose axis inclined (“oblique”) to the rotation axis, is known as the *oblique rotator model*.

The simplest oblique rotator is a magnetic dipole whose axis is inclined at some angle β to the rotation axis, which of course is also inclined by an angle i to the line of sight. For this simplest model, to fully specify everything, we must provide a value for i , one for β , and the polar strength of the dipole B_d . This makes three parameters. But a simple sinusoidal variation of $\langle B_z \rangle$ only provides two constraints, for example the mean value of $\langle B_z \rangle$ and the amplitude of variation, or the minimum and maximum values of $\langle B_z \rangle$. Other information such as the time of maximum field provides nothing useful for the three parameters we need. In order to use the variation of $\langle B_z \rangle(t)$ (known in the trade as a “magnetic curve”) to determine the parameters uniquely, it is necessary to determine i , usually from $v_e \sin i$ and the stellar radius. To define this model better, or to use one with more parameters, we need more information about the field.

4.4 The mean field modulus and better Ap magnetic models

Another kind of information about the field that is sometimes available, and very useful if it is, is the mean value of the field strength $\langle |B| \rangle$, averaged over the

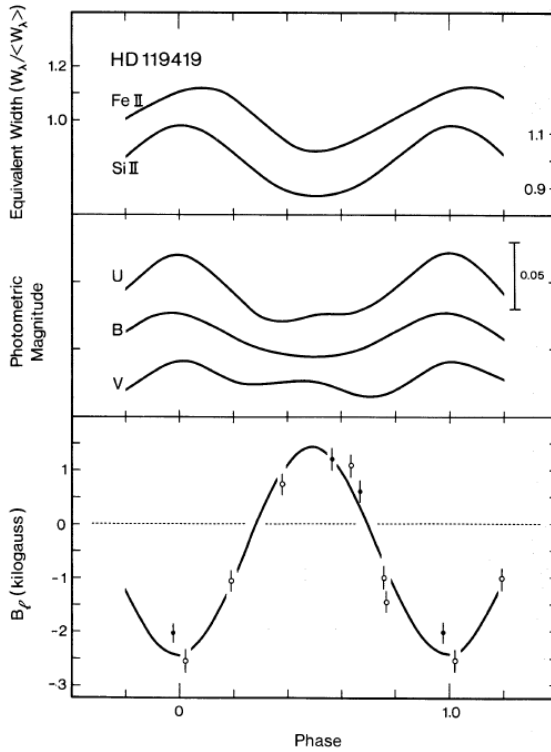


Fig. 6. Variations observed in the magnetic Ap star HD 119419 as a function of phase through the 2.60 d period. The curves show (from the top) the variations of equivalent width of Fe and Si lines, of brightness in the Johnson UBV bands, and of $\langle B_z \rangle$.

visible stellar hemisphere, and known as the *mean field modulus* or *mean surface field* B_s . This number is accessible in stars in which the value of $v_e \sin i$ is small enough, and the field large enough, that actual line splitting into components (or at least broadening of the most Zeeman-sensitive lines) is observable. This usually requires a $v_e \sin i$ value of at most a few km s^{-1} , and a field strength of some kG. For stars for which such splitting (or excess broadening) is detectable, the basic measurement method is to measure the wavelength separation between the pi and sigma components (or between the two sigma components) and use Eq. 2.7 to determine the mean field modulus. An example of the kind of splitting that could be measured is shown in Fig. 3 in the next chapter; the mean field modulus in this star is about 34 kG! The value of B_s sometimes (but not always) varies roughly sinusoidally too.

With two more constraints from measurements of B_s (say maximum and minimum values during one rotation), we can not only constrain the three parameters

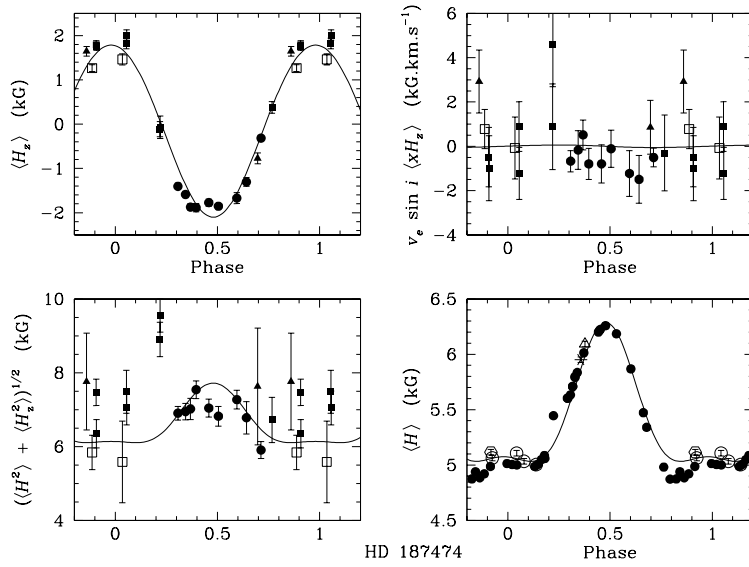


Fig. 7. Models of several field moments measured for HD 187474. The upper left panel shows $\langle B_z \rangle$, and the lower right panel shows B_s , with data superposed on a fit using co-linear dipole, quadrupole, and octupole. (There is enough information in the data set to constrain one additional parameter.)

of the dipole rotator, but add a second field component, which might for example be a linear quadrupole field aligned with the dipole, for which we need only specify one more polar field strength. This additional field component would allow us to bunch the field lines together at one pole and spread them apart at the other, creating a strong pole and a weak pole, a situation frequently required by the data. A particularly attractive aspect of this kind of approximate modelling is that it enables us to obtain a qualitative picture of the overall field structure *without* detailed computation of line profiles. An example of such modelling, from Landstreet & Mathys 2000, is shown in Fig. 4.4.

Such simple modelling nevertheless allows us to obtain some rather important insights into the nature of the magnetic fields of Ap stars.

- The fact that Zeeman-split spectral lines mostly have well-defined sigma and pi components, and that in lines for which the splitting pattern happens to have no component at zero displacement (i.e. the multiple pi components all separate from the zero-field wavelength), indicate that the fields of the Ap stars are fairly homogeneous. These stars do not seem to have the mixture of regions of fairly strong field and other regions essentially free of field that characterise the field structure of solar-type stars.

- Typically, the largest values of $\langle B_z \rangle$ is of the order of 0.2 or 0.3 of the value of B_s . This is only possible if the field has a globally dipolar topology, with most field lines entering the star on one hemisphere and exiting on the other. A more complex field structure would reduce $\langle B_z \rangle$ to a much smaller fraction of B_s .
- In general, in stars where it is possible to measure B_s , the two magnetic poles do not have equal characteristic field strengths. One pole is usually stronger than the other. This is probably connected with the fact (at first rather surprising) that elements which have a patchy distribution may have a maximum abundance near one pole and a minimum near the other: if the poles are “different”, the abundance patterns could be too.

5 Conclusions

We find that the physics of the Zeeman effect provides us with several robust tools with which to detect and measure the magnetic fields of stars. Such fields have been known for many years on the Sun and on the Ap stars. The solar field is strongly structured on a small length scale, and strongly variable on a short time scale. In contrast, the fields of Ap stars seem to be structured rather simply, and are constant in time in their intrinsic structure over the star; no real changes seem to occur, only the periodic changes due to stellar rotation. We suspect that these two types of fields have rather different origins, which we will discuss in Chapter 3.

References

- Arnaud, J. & Meunier, N. 2003, editors, *“Magnetism and Activity of the Sun and Stars*, EAS Pubs. Series No. 9 (Paris, EDP Sciences)
- Babcock, H. W. 1947, ApJ 105, 105
- Babcock, H. W. 1958a, ApJS 3, 141
- Babcock, H. W. 1958b, ApJ 128, 228
- Bagnulo, S., Szeifert, T., Wade, G. A., Landstreet, J. D. & Mathys, G. 2002, A&A 389, 191
- Balona, L., Henrichs, H. F. & Medupe, R. 2003, editors, *“Magnetic Fields in O, B and A Stars”*, ASP Conf. Series No. 305 (San Francisco: Astronomical Society of the Pacific)
- Bransden, B. H. & Joachain, C. J. 1983, *“Physics of Atoms and Molecules”*, (London: Longman) ch. 8
- Bray, R. J. & Loughhead, R. E. 1964, *“Sunspots”*, (New York: Wiley)
- Eisberg, R. & Resnick, R. 1985, *“Quantum Mechanics of Atoms, Molecules, Solids, Nuclei, and Particles”*, (New York: John Wiley & Sons), ch. 10
- Hale, G. E. 1908, ApJ 28, 315
- Krtićka, J., Mikulášek, Z., Zverko, J. & Žižňovský, J. 2007, A&A 470, 1089
- Landstreet, J. D. 1982, ApJ 258, 639

- Landstreet, J. D. & Mathys, G. 2000, *A&A* 359, 213
- Mathys, G., Solanki, S. K. & Wickramasinghe, D. T. 2001, editors, *"Magnetic Feilds Across the Hertzsprung-Russell Diagram"*, ASP Conf. Series No. 248 (San Francisco: Astronomical Society of the Pacific)
- Mestel, L. 1999, *"Stellar Magnetism"*, (Oxford: Clarendon Press)
- Moore, C. *"Atomic Energy Levels"*, 3 vols., NBS Circular 467 (Washington: NBS)
- Schiff, L. I. 1955, *"Quantum Mechanics"*, (New York: McGraw-Hill)
- Wielebinski, R. & Beck, R. 2005, editors, *"Cosmic Magnetic Fields"* (Berlin: Springer-Verlag)
- Zverko, J., Žižňovský, J., Adelman, S. J. & Weiss, W. W. 2005, editors, *"The A-Star Puzzle"*, IAU Symposium No. 224 (Cambridge: Cambridge University Press)